

Minimal cytosolic iron-sulfur cluster assembly machinery of *Giardia intestinalis* is partially associated with mitosomes

Jan Pyrih,^{1†} Eva Pyrihová,¹ Martin Kolísko,^{2‡}
Darja Stojanová,¹ Somsuvro Basu,^{3§}
Karel Harant,¹ Alexander C. Haindrich,^{3,4}
Pavel Doležal,¹ Julius Lukeš,^{3,4,5} Andrew Roger^{2,5}
and Jan Tachezy^{1*}

¹Department of Parasitology, Charles University in Prague, Vestec 252 42, Czech Republic.

²Centre for Comparative Genomics and Evolutionary Bioinformatics, Department of Biochemistry and Molecular Biology, Dalhousie University, Halifax, NS B3H 4R2, Canada.

³Institute of Parasitology, Biology Centre, České Budějovice, Budweis 37005, Czech Republic.

⁴Faculty of Sciences, University of South Bohemia, České Budějovice, Budweis 37005, Czech Republic.

⁵Canadian Institute for Advanced Research, Toronto, ON M5G 1Z8, Canada.

Summary

Iron-sulfur (Fe-S) clusters are essential cofactors that enable proteins to transport electrons, sense signals, or catalyze chemical reactions. The maturation of dozens of Fe-S proteins in various compartments of every eukaryotic cell is driven by several assembly pathways. The ubiquitous cytosolic Fe-S cluster assembly (CIA) pathway, typically composed of eight highly conserved proteins, depends on mitochondrial Fe-S cluster assembly (ISC) machinery. *Giardia intestinalis* contains one of the smallest eukaryotic genomes and the mitosome, an extremely reduced mitochondrion. Because the only pathway known to be retained within this organelle is the synthesis of Fe-S clusters mediated by ISC machinery, a likely function of the mitosome is to cooperate with the CIA pathway. We investigated the cellular localization of

CIA components in *G. intestinalis* and the origin and distribution of CIA-related components and Tah18-like proteins in other Metamonada. We show that orthologs of Tah18 and Dre2 are missing in these eukaryotes. In *Giardia*, all CIA components are exclusively cytosolic, with the important exception of Cia2 and two Nbp35 paralogs, which are present in the mitosomes. We propose that the dual localization of Cia2 and Nbp35 proteins in *Giardia* might represent a novel connection between the ISC and the CIA pathways.

Introduction

Iron-sulfur (Fe-S) clusters are important cofactors found in a variety of proteins in each and every extant cell. The ability of these ancient cofactors to transfer electrons is essential for near-ubiquitous processes such as respiration, photosynthesis, isoprenoid biosynthesis, DNA metabolism and translation (Netz *et al.*, 2014; Tanaka *et al.*, 2015). The Fe-S cluster assembly is performed by dedicated machineries in several cellular compartments. The iron sulfur cluster (ISC) pathway is present in mitochondria, the sulfur mobilization pathway is confined to plastids, and the cytosolic iron-sulfur cluster assembly (CIA) is found in the cytosol. The CIA pathway is required for the maturation of all cytosolic and nuclear Fe-S cluster-containing proteins (Stehling *et al.*, 2012; Stehling *et al.*, 2013; Netz *et al.*, 2014). All eight components of this pathway identified thus far (Tah18, Dre2, Nbp35, Cfd1, Nar1, Cia1, Cia2 and MMS19) appear to be present in most eukaryotes. Initially, a transient [4Fe-4S] cluster is assembled on a cytosolic hetero-tetrameric scaffold complex composed of Cfd1 and Nbp35 (Hausmann *et al.*, 2005; Netz *et al.*, 2007, 2012), where it is coordinated by the bridging of two cysteine residues of Nbp35 to another two cysteines on Cfd1. In addition, Nbp35 binds another stable [4Fe-4S] cluster at its N terminus (Netz *et al.*, 2012). The transient cluster is then transferred to apoproteins with

Accepted 21 August, 2016. *For correspondence E-mail tachezy@natur.cuni.cz; Tel. (+420) 325 873 144. Present addresses: [†]School of Biosciences, University of Kent, CT2 7NJ, United Kingdom; [‡]Department of Botany, University of British Columbia, Vancouver, V6T 1Z4, Canada [§]Institut für Zytobiologie, Philipps-Universität Marburg, Marburg, 35032, Germany.

the assistance of the hydrogenase-like protein Nar1 (Balk *et al.*, 2004) and the CIA targeting complex formed by Cia1, Cia2 and MMS19 (Balk *et al.*, 2005; Gari *et al.*, 2012; Luo *et al.*, 2012; Stehling *et al.*, 2012). Coprecipitations and functional studies have revealed that the Cia1, Cia2 and MMS19 components are dedicated to the maturation of cytosolic and nuclear FeS proteins involved mainly in DNA metabolism (Stehling *et al.*, 2012). Although a role of Cia2, a small protein containing the DUF59 domain with a highly conserved reactive cysteine residue (Weerapana *et al.*, 2010), in cluster loading on a subset of cytosolic and nuclear Fe-S proteins has been described (Stehling *et al.*, 2012), its precise function remains unknown.

Furthermore, an electron transfer chain composed of the NADPH-dependent diflavin oxidoreductase Tah18 and the Fe-S carrying Dre2 is required for the assembly of the [4Fe-4S] cluster on Nbp35 (Zhang *et al.*, 2008; Netz *et al.*, 2010). It was demonstrated that Tah18 enables electron transfer from NADPH to Dre2, from which electrons are then transferred to Nbp35 (Netz *et al.*, 2010). Interestingly, several other alternative functions unrelated to Fe-S cluster synthesis, such as the control of mitochondrial integrity and cellular death (Vernis *et al.*, 2009), and nitric oxide synthesis (Nishimura *et al.*, 2013), as well as involvement in the synthesis of the diferric-tyrosyl radical cofactor of ribonucleotide reductase (Zhang *et al.*, 2014), were suggested for the Tah18 and Dre2 proteins in yeast. It is noteworthy that Tah18 is highly similar to cytochrome p450 reductase and methionine synthase reductase, the shared features being similar length, an NADP⁺ binding site and FMN and FAD redox centers, with the latter containing the CPR domain derived from the cytochrome p450 reductase-like domain (Netz *et al.*, 2010; Jedelsky *et al.*, 2011). Moreover, this domain is also part of several fusion proteins, such as nitric oxide synthase in metazoans and pyruvate:NADP⁺ oxidoreductase (PNO) in various protists (Rotte *et al.*, 2001; Iyanagi *et al.*, 2012).

In yeasts, human and plants, it has been shown that Fe-S cluster formation via the CIA pathway is dependent on the export of a still unknown sulfur-containing compound likely generated in mitochondria by the ISC machinery (Leighton and Schatz, 1995; Kispal *et al.*, 1999; Lange *et al.*, 2001; Mühlenhoff *et al.*, 2004; Netz *et al.*, 2014). The Atm1 and Erv1 proteins located in the inner mitochondrial membrane and the intermembrane space, respectively, were implicated in the export of this compound from the organelle (Kispal *et al.*, 1999; Lange *et al.*, 2001). Additionally, thiol-containing glutathione, an indispensable connection between the ISC and CIA pathways (Sipos *et al.*, 2002; Srinivasan *et al.*, 2014), is bound to Atm1 in the form of a cofactor and stimulates its ATPase activity (Kuhnke *et al.*, 2006; Srinivasan

et al., 2014). However, the exact mechanism of the export across the two mitochondrial membranes of this elusive sulfur-containing precursor required by the CIA pathway remains unknown (Lill *et al.*, 2015).

Although our understanding of the CIA machinery in yeast, human and plant cells is increasing (Netz *et al.*, 2014), only very limited information is available about how Fe-S clusters are assembled in the cytosol of anaerobic protists. Several components of the CIA machinery, such as Nbp35, Nar1, Cia1 and Cia2, are highly conserved across eukaryotes (Basu *et al.*, 2013; Tsaousis *et al.*, 2014), whereas Dre2 and Erv1 have been proposed to be absent in anaerobes (Basu *et al.*, 2013). Moreover, although various anaerobic protists possess proteins with a CPR domain, similar to Tah18, their classification and functional characterization are challenging, because knock-down techniques have not typically been established for these organisms. Furthermore, human Tah18 protein was shown to interact with cytochromes *in vitro* similarly to cytochrome p450 reductase (Olteanu and Banerjee, 2003), casting doubt over the suitability of knock-in techniques to distinguish between these two proteins. To identify the Tah18 homologs, phylogenetic analysis was used to classify the CPR domain-containing proteins, although in anaerobes such as *Blastocystis* and *Giardia* resolution was limited due to their extensive divergence (Tsaousis *et al.*, 2014).

As an adaptation to anaerobic environments and a parasitic lifestyle, *Giardia intestinalis*, a member of the phylum Metamonada, has reduced its mitochondria into mitosomes (Tovar *et al.*, 2003; Doležal *et al.*, 2005). The only pathway identified within this organelle to date is ISC-mediated Fe-S cluster synthesis (Jedelsky *et al.*, 2011; Martincová *et al.*, 2015). Furthermore, *G. intestinalis* possesses a minimalistic nuclear genome with only a few introns (Morrison *et al.*, 2007), as well as simplified machineries for DNA replication, transcription, RNA processing, and most metabolic pathways (Morrison *et al.*, 2007). The Atm1, Erv1 and Dre2 proteins are prominently absent from the *G. intestinalis* genome, whereas Nbp35, Nar1, Cia1 and Cia2 have been identified (Tsaousis *et al.*, 2014). The CPR domain-containing GiOR-1 and GiOR-2 proteins are putative orthologs of Tah18 (Jedelsky *et al.*, 2011; Basu *et al.*, 2013; Tsaousis *et al.*, 2014). Interestingly, GiOR-1, a possible reductase of cytosolic *b₅* cytochromes (Pyrih *et al.*, 2014), was previously identified in the mitosome, whereas GiOR-2 is associated with heretofore unidentified vesicles (Jedelsky *et al.*, 2011).

It is noteworthy that in *G. intestinalis* many proteins are highly divergent (Morrison *et al.*, 2007; Dagley *et al.*, 2009), which limits or even hinders homology searches (Dagley *et al.*, 2009; Martincová *et al.*, 2015). However,

related free-living metamonads, such as *Trimastix* or *Carpediemonas*, tend to constitute shorter branches in molecular phylogenies and consequently appear to be less diverged and more suitable for this approach (Kolísko *et al.*, 2010; Takishita *et al.*, 2012).

Here, we show that Tah18, Dre2, Erv1, Atm1 and MMS19 are likely absent from metamonads, whereas Cfd1 could not be identified by homology searches in *G. intestinalis* and *Spironucleus* but is present in *Carpediemonas* and *Trichomonas vaginalis*. Moreover, we provide evidence that GiOR-1 and GiOR-2 likely perform cellular roles unrelated to those of Tah18. The cytosolic localization of Cia1, Nar1 and one paralog of Nbp35 was anticipated; however, the dual mitochondrial and cytosolic localization of the other paralogs of Nbp35 and Cia2 was surprising.

Results

CIA components in metamonads

We performed homology searches for the CIA components in the genomes of metamonads *G. intestinalis*, *T. vaginalis* and *Spironucleus salmonicida* and in the EST data of other metamonads for which genomes are not available. The Nbp35, Nar1, Cia1 and Cia2 genes were present in all these protists (Fig. 1). The absence of some of core components in *Trimastix marina* (isolate PCT), *Spironucleus vortens*, *Ergobibamus cyprinoides* and *Carpediemonas*-like organism (CLO NY171) is most likely caused by insufficient sequence data coverage. Dre2 and MMS19 are most likely absent in metamonads, with the exception of a putative divergent MMS19 homolog in *T. marina* (Fig. 1). The Cfd1 protein is the only CIA component that showed a varied distribution across metamonads, as it was identified in *T. vaginalis*, *C. membranifera*, CLO NY171 and *Chilomastix cuspidata*, whereas it could not be identified by homology searches in *G. intestinalis* and *S. salmonicida* (Fig. 1). Because the latter two genera are more derived (Takishita *et al.*, 2012), we propose that Cfd1 was present in the ancestor of all metamonads and was possibly lost only secondarily. Next, we searched for the CPR domain-containing proteins, possible Tah18 homologs. In addition to the GiOR proteins in *G. intestinalis*, similar Tah18-like proteins were identified in *Trepomonas* sp. (isolate PC1), *Dysnectes brevis*, and CLO NY171 (Fig. 1). Interestingly, in *T. vaginalis*, *C. membranifera*, *T. marina*, and *C. cuspidata*, we were able to identify only fusion genes of the CPR domain with hydrogenase. In *D. brevis*, both genes carrying the fusion hydrogenase and only the CPR domain are present. Although the presence of ABC transporters similar to the ISC and

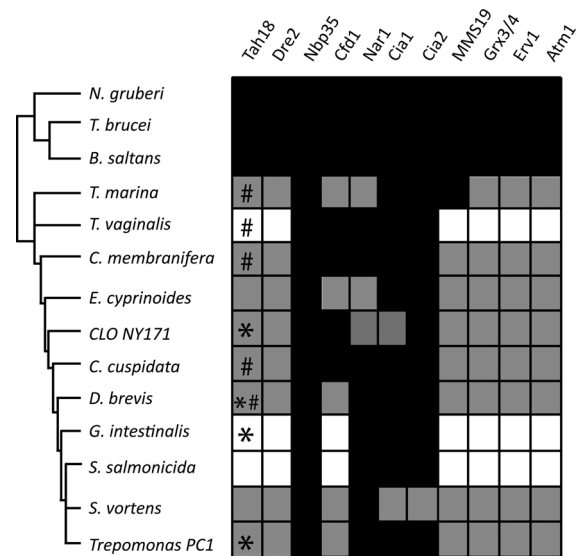


Fig. 1. Distribution of CIA machinery components in metamonads. The complete CIA pathway is present in selected members of the Kinetoplastea (*Trypanosoma brucei*, *Bodo saltans*) and Heterolobosea (*Naegleria gruberi*) groups. In metamonads, this pathway is reduced to a minimal set of proteins: Nbp35, Cfd1, Nar1, Cia1 and Cia2. The presence of an ortholog in the genome is denoted by black shading. The absence is indicated in white. Gray indicates that the gene is absent in the available EST database. For Tah18-like orthologs, the presence of similarly organized proteins or fusion with a hydrogenase-like domain is indicated by an asterisk or hash sign, respectively. Relationships between different eukaryotic groups is based on the current consensus (Takishita *et al.*, 2012).

CIA linking proteins Erv1 and Atm1 was previously suggested in the *G. intestinalis* mitosome (Jedelsky *et al.*, 2011), we were unable to identify any putative homologs of these two proteins.

Localization of CIA pathway components in Giardia

In the *G. intestinalis* genome, Nar1, Cia1 and Cia2 are encoded by single-copy genes, whereas Nbp35 is present in three similar copies, herein labeled Nbp35-1, Nbp35-2 and Nbp35-3. To investigate their subcellular localization, all these CIA components were expressed with a C-terminal HA-tag. In parallel, specific antibodies against the HA-tag or target proteins were used for immunofluorescence microscopy and probing of subcellular fractions.

To corroborate the previously observed mitochondrial localization of the HA-tagged GiOR-1 (Jedelsky *et al.*, 2011), polyclonal antibody was raised against this protein. Indeed, all specific signals were localized in the mitosomes (Fig. 2). Both immunofluorescence microscopy and western blot analysis of subcellular fractionation indicated cytosolic localization of Nar1, Cia1 and Nbp35-3 (Fig. 2). Interestingly, immunofluorescence

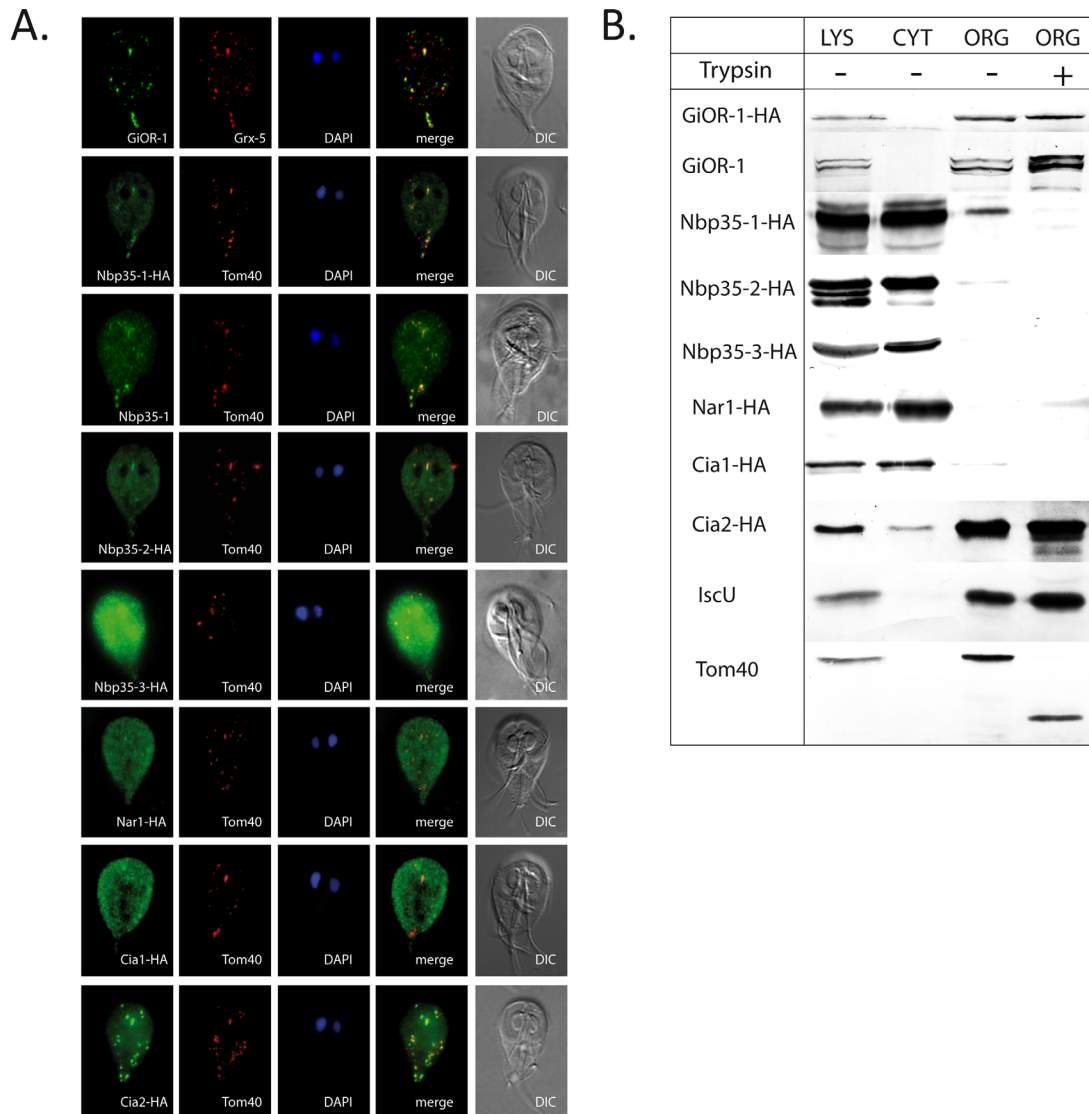


Fig. 2. Subcellular distribution of CIA pathway components in *G. intestinalis*

A. Localization of proteins of CIA pathway in *G. intestinalis* using immunofluorescence microscopy. α -HA rat antibody was used to detect HA-tagged proteins (green signal). Specific α -GiOR-1 rabbit and anti-Nbp35-1 rat polyclonal antibodies were used to detect GiOR-1 and Nbp35-1, respectively, in wild-type cells. Grx5, Tom40 and IscU were used as markers for the mitochondrial outer membrane and matrix, respectively. The proteins were detected by polyclonal rabbit α -Tom40 and α -IscU antibodies. Nuclei were stained with DAPI (blue). DIC, differential interference contrast.

B. Western blot analysis of subcellular fractions. The same primary antibodies indicated above were used. Trypsin treatment of the organellar fraction is indicated by “+” (protein protection assay). LYS, cell lysate; CYT, cytosol; ORG, mitosome-containing organellar fraction.

analysis of Cia2 revealed its partial association with the mitosomes (Fig. 2A), an observation further confirmed by subcellular fractionation, which clearly localized a portion of the Cia2 signal within the organellar fraction (Fig. 2B). Moreover, protein protection assay using trypsinization of the organellar sample revealed that Cia2 is present inside of the organelles. Similarly, Nbp35-1 and Nbp35-2 possess dual cytosolic and mitosomal localization, as observed by immunofluorescence. Moreover, a faint band and a barely detectable band corresponding

to Nbp35-1 and Nbp35-2, respectively, were associated with the organellar fraction. However, following trypsinization of the samples, both Nbp35-1 and Nbp35-2 bands were lost (Fig. 2B), similarly to the integral outer mitosomal membrane marker protein Tom40, the cytosolic part of which was digested upon the addition of trypsin (Martinová *et al.*, 2015; Fig. 2B). This finding suggests that both Nbp35-1 and Nbp35-2 most likely have dual localization, being distributed in the cytosol and associated with the outer mitosomal membrane.

The dual localization of Nbp35-1 was further confirmed using the α -Nbp35-1 antibody (Fig. 2A). To address the possibility of its interaction with mitosome-associated CIA components, the localization of GiOR-1 was investigated in greater detail. Together with the results from immunofluorescence, a protease protection assay performed using the α -GiOR-1 antibody convincingly showed that GiOR-1 is an inner mitosomal protein (Fig. 2A and B).

Intramitosomal distribution of Cia2 and GiOR-1

No technique for mitosome subfractionation is currently available. To better understand the exact topology of Cia2 and GiOR-1 within the mitosome, an *in vivo* biotinylation assay followed by precipitation of interacting proteins, a technique recently established for *G. intestinalis* (Martincová *et al.*, 2015), was performed. Briefly, the protein of interest is expressed as a fusion protein with a biotin acceptor peptide (BAP) in a cell line coexpressing cytosolic biotin ligase (cBirA). cBirA biotinylates BAP-tagged proteins that are in the cytosol as well as proteins that are post-translationally targeted to mitosomes (Martincová *et al.*, 2015). Thus, the protein of interest is biotinylated *in vivo*; the sample is treated with dithiobis succinimidyl propionate (DSP), a membrane-permeable cross-linking reagent; and the complex composed of the protein of interest and its interacting partners is purified using streptavidin-coupled magnetic beads. The samples are washed under highly stringent condition of 2% sodium dodecyl sulfate and analyzed by mass spectrometry. The same procedure is performed with wild-type *Giardia* and cells overexpressing BirA protein only, and proteins identified in these negative controls are subtracted from the dataset that was obtained with the lineage expressing BAP-tagged proteins (Supporting Information Table S1).

The majority of the proteins identified upon the purification of putative interacting partners of GiOR-1 are homologs of mitochondrial matrix proteins (Fig. 3A). These proteins are involved in mitochondrial protein import and maturation (Hsp70, Hsp60, Tim44 and giardial processing peptidase) or the ISC machinery (IscS, Nfu and glutaredoxin 5).

In contrast, coprecipitation of Cia2 from the mitosome-containing fraction did not reveal any known mitosomal matrix proteins among its putative interaction partners (Fig. 3B). However, all identified proteins were previously found to coprecipitate with integral outer mitosomal membrane proteins Tom40 and GiMOMP35 (Martincová *et al.*, 2015; Fig. 3B). Together with the finding that Cia2 is present within the mitosome (Fig. 2B), the identification of its interacting partners strongly

points toward localization of the mitosomal fraction of Cia2 in the intermembrane space.

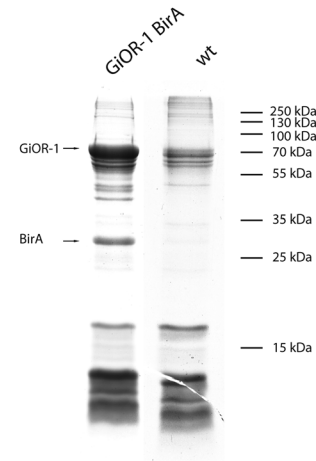
Functional characterization of GiOR-1 and GiOR-2 in Trypanosoma brucei

To functionally address the putative relatedness between the GiOR and Tah18 proteins (GiOR-1, and GiOR-2 displayed 17.5%, and 19% amino acid sequence identities when compared with *T. brucei* Tah18, respectively), the ability of both GiOR proteins to rescue the Tah18-dependent activity in the CIA pathway of *T. brucei* was tested. In the procyclic stage of *T. brucei*, RNAi-mediated depletion of either *TbTah18* or *TbDre2* did not result in a growth phenotype, likely because of the insufficient downregulation of the target protein (Basu *et al.*, 2014). Nevertheless, the essentiality of these proteins in the CIA machinery was demonstrated by the RNAi double knock-down of *TbTah18* and *TbDre2* (Basu *et al.*, 2014). The expression of HA-tagged GiORs in *T. brucei* lacking both *TbTah18* and *TbDre2* resulted in a slight rescue of the growth phenotype (Fig. 4A). Taken together, growth of both rescue cell-lines is ameliorated compared with that of the *TbTah18-TbDre2* double RNAi mutant line (the cumulative density of the *TbTah18-TbDre2* double RNAi-non-induced strain was below 10 log cells/ml after 10 days of RNAi induction, but for the GiOR-1 or GiOR-2 rescue strains the growth attained 10 log cells/ml or above, respectively) (Fig. 4A). Next, we wondered whether the Fe-S cluster-dependent activity of a cytosolic enzyme has been rescued by expression of the heterologous protein from *Giardia*. For this purpose, the activity of the cytosolic enzyme aconitase that carries [4Fe-4S] clusters was measured following a protocol described elsewhere (Long *et al.*, 2011). Indeed, a strong rescue of its activity was observed in trypanosomes expressing either GiOR-1 or GiOR-2, where >50 or 40% revival was achieved, respectively (Fig. 4B). As an internal control, the measurement of mitochondrial aconitase activity showed that in this cellular compartment it remained unaffected (Fig. 4B).

The function of Tah18 is dependent on the interaction with Dre2 within the same cellular compartment (cytosol); however, in *Giardia*, GiOR-1 is present in mitosomes, whereas GiOR-2 is in multiple vesicles of unclear character (Jedelsky *et al.*, 2011). Therefore, we investigated localization of HA-tagged GiOR proteins in *T. brucei*. Both proteins were present exclusively in the cytosolic cellular fraction (Fig. 4C), which is in agreement with their ability to partially complement the *TbTah18-TbDre2* double RNAi knock down. However, the difference in the cellular localization of GiOR

A.

Name of the protein	G.I. number	TM	UP	Pam 18	Tim 44	Hsp 70	Tom 40	Momp 35	Cia 2
GiOR-1	GL50803_91252	0	7						
Hsp70	GL50803_14581	0	9						
Cpn60	GL50803_103891	0	8						
IscS	GL50803_14519	0	4						
GPP	GL50803_9478	0	3						
Glutaredoxin 5	GL50803_2013	0	3						
Tim44	GL50803_14845	0	2						
Hypothetical	GL50803_3491	0	2						
Nfu	GL50803_32838	0	2						
Ferredoxin	GL50803_27266	0	2						
Rhodanese like	GL50803_27910	0	2						
Hypothetical	GL50803_3582	0	2						



B.

Name of the protein	G.I. number	TM	UP	Pam 18	Tim 44	Hsp 70	Tom 40	Momp 35	GiOR 1
Cia2	GL50803_8819	0	7						
Hypothetical	GL50803_17249	0	7						
Hypothetical	GL50803_113603	0	4						
Carboxy peptidase (putative)	GL50803_10976	0	3						
Multidrug MFS transporter	GL50803_8444	11	3						
Hypothetical	GL50803_94542	1	2						
Hypothetical	GL50803_7723	0	2						
Myeloid leukemia factor	GL50803_16424	0	2						
Hypothetical	GL50803_16648	0	2						

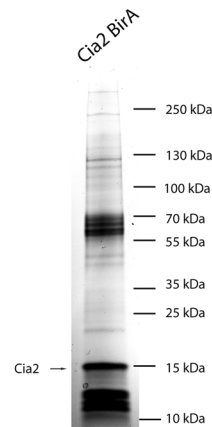


Fig. 3. Identification of GiOR-1 and Cia2 interacting proteins in mitosome.

A1. List of proteins coprecipitated with GiOR-1. GPP, *Giardia* processing peptidase; IscS, cysteine desulfurase; Thioredoxin reductase, Thioredoxin reductase; S/T kinase, Serine/Threonine kinase. A2. A representative SDS-PAGE analysis of proteins coprecipitated with GiOR-1 is displayed. GiOR-1 was biotinylated by cytosolic BirA (GiOR-1 BirA). wt, control sample of proteins precipitated from wild-type cells. Following SDS-PAGE, the proteins were submitted to mass spectrometry.

B1. List of proteins co-precipitated with mitosomal biotinylated Cia2 protein. B2. Representative SDS-PAGE analysis of proteins coprecipitated with biotinylated Cia2 (Cia2 BirA), and the control sample (wt).

TM, number of transmembrane domains predicted by TMHMM transmembrane prediction software; UP, number of unique peptides identified by mass spectrometry analysis for a given protein. The presence of protein precipitated with GiOR-1 (A) and Cia2 (B) in the interactome of Pam18, Tim44, Hsp70, Tom40, Momp35 (Martincová *et al.*, 2015) and Cia2, and GiOR-1 (this study) is denoted in black; absence is indicated in white. Acc. number, accession number according to GiardiaDB (giardiadb.org).

proteins between *G. intestinalis* and *T. brucei* is surprising. Particularly, the mode of the protein targeting to mitochondria and mitosomes via N-terminal targeting presequences have been shown to be conserved (Doležal *et al.*, 2005). In GiOR-1, there is not obvious N-terminal targeting presequence (Jedelsky *et al.*, 2011), although PSORT II software predicted a putative cleavage site for the mitochondrial processing peptidase between 29th and 30th amino acid residues. Therefore, we tested the cellular localization of the truncated GiOR-1 with deleted 29 amino acid residues at the N-terminus. The truncated GiOR-1 was associated with mitosomes and significant part of the protein was found inside of these organelles (Supporting Information

Figure S1). These results suggest that GiOR-1 is targeted to the mitosomes via internal targeting signal, which is not recognized in *T. brucei*.

Phylogeny-based classification of CPR domain-containing proteins in metamonada

To assess the evolution of Tah18-like proteins in Metamonada, we performed a phylogenetic analysis using the CPR domains of various proteins encoded by the representatives of all eukaryotic supergroups. The phylogenetic analysis revealed that the Tah-18-like proteins, including GiOR-1 and GiOR-2, clustered with the CPR-hydrogenase fusion proteins of metamonads and

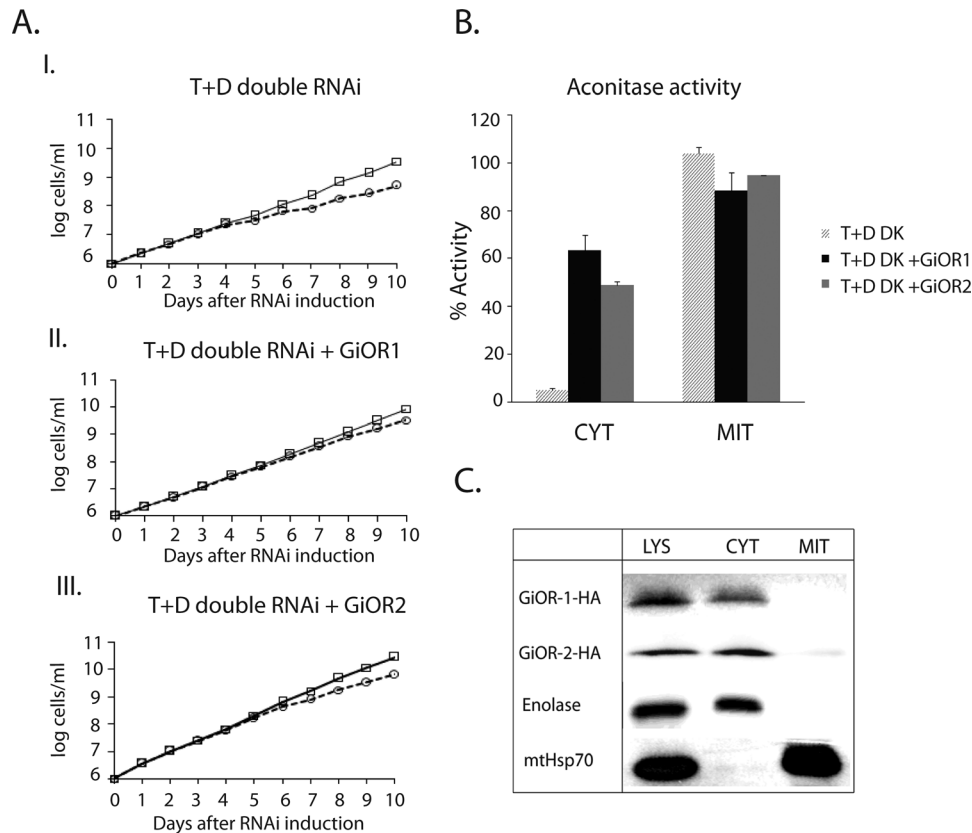


Fig. 4. GiOR rescue experiment in *Trypanosoma brucei*

A. Tah18 and Dre2 knock-down phenotype can be rescued by expressing GiOR-1 and GiOR-2 proteins. A. Growth of *T. brucei* RNAi cell lines is partially rescued by expression of the GiOR proteins. The cumulative density of the cells is indicated by a solid line (non-induced) or broken line (induced). I. The *TbTah18-TbDre2* double RNAi strain presents a moderate growth effect upon RNAi induction. II & III. The double-RNAi-generated growth effect is partially rescued by the GiOR1 and GiOR2 proteins, respectively. Standard deviations calculated for each time point were below ± 0.5 log cell/ml.

B. Aconitase activity is restored in the cytosol of *T. brucei* RNAi cell lines upon expression of GiOR proteins. Measurement was performed after 6 days of RNAi induction. % Activity expresses relative activity determined in RNAi induced cells when the activity in noninduced cells have been set as 100%. Error bars represent standard deviation calculated from three independent experiments. *TbTD*, *TbTah18-TbDre2* double RNAi inducible strain; CYT, cytosolic fraction; MIT, mitochondrial fraction.

C. Cellular localization of GiOR proteins in the *TbTah18-TbDre2* double RNAi strain. HA-tagged GiOR proteins were detected in cellular fractions using western blot analysis. Enolase, and mitochondrial Hsp70 were used as cytosolic, and mitochondrial marker proteins, respectively. LYS, cellular lysate; CYT, cytosolic fraction; MIT, mitochondrial fraction.

Mastigamoeba balamuthi (Nývltová *et al.*, 2015), whereas the Tah18 homologs in all other organisms formed a distinct branch (Fig. 5).

The hydrogenase domain of the CPR-hydrogenase fusion protein in *T. vaginalis* was suggested to correspond to the hydrogenase-like protein Nar1 (Basu *et al.*, 2013). Indeed, similarly to Nar1, the *T. vaginalis* protein possesses a mutated HC1 site for H-cluster binding and therefore likely does not function as a standard hydrogenase (Peters *et al.*, 1998; Basu *et al.*, 2013); however, no corresponding phylogenetic analysis has been performed to date. Therefore, we searched for the evolutionary origin of the N-terminal hydrogenase-like domain of the CPR-hydrogenase fusion proteins in metamonads. The obtained results indicate that these proteins are derived from hydrogenases and not from Nar1

(Supporting Information Figure S2). In contrast to the *T. vaginalis* homologue, the motif for H cluster binding (TSCCP) is present in CPR-hydrogenase fusion proteins of other metamonads (Supporting Information Figure S2).

Discussion

Distribution of CIA pathway components in metamonada

Searches for components of the CIA pathway in the genomes of model excavate protists, such as *T. brucei*, *Naegleria gruberi* and *Bodo saltans*, revealed a complete set of proteins (Basu *et al.*, 2014; Tsousis *et al.*, 2014; Jackson *et al.*, 2016; Fig. 1). In contrast, the same search for CIA homologs in Metamonada, which

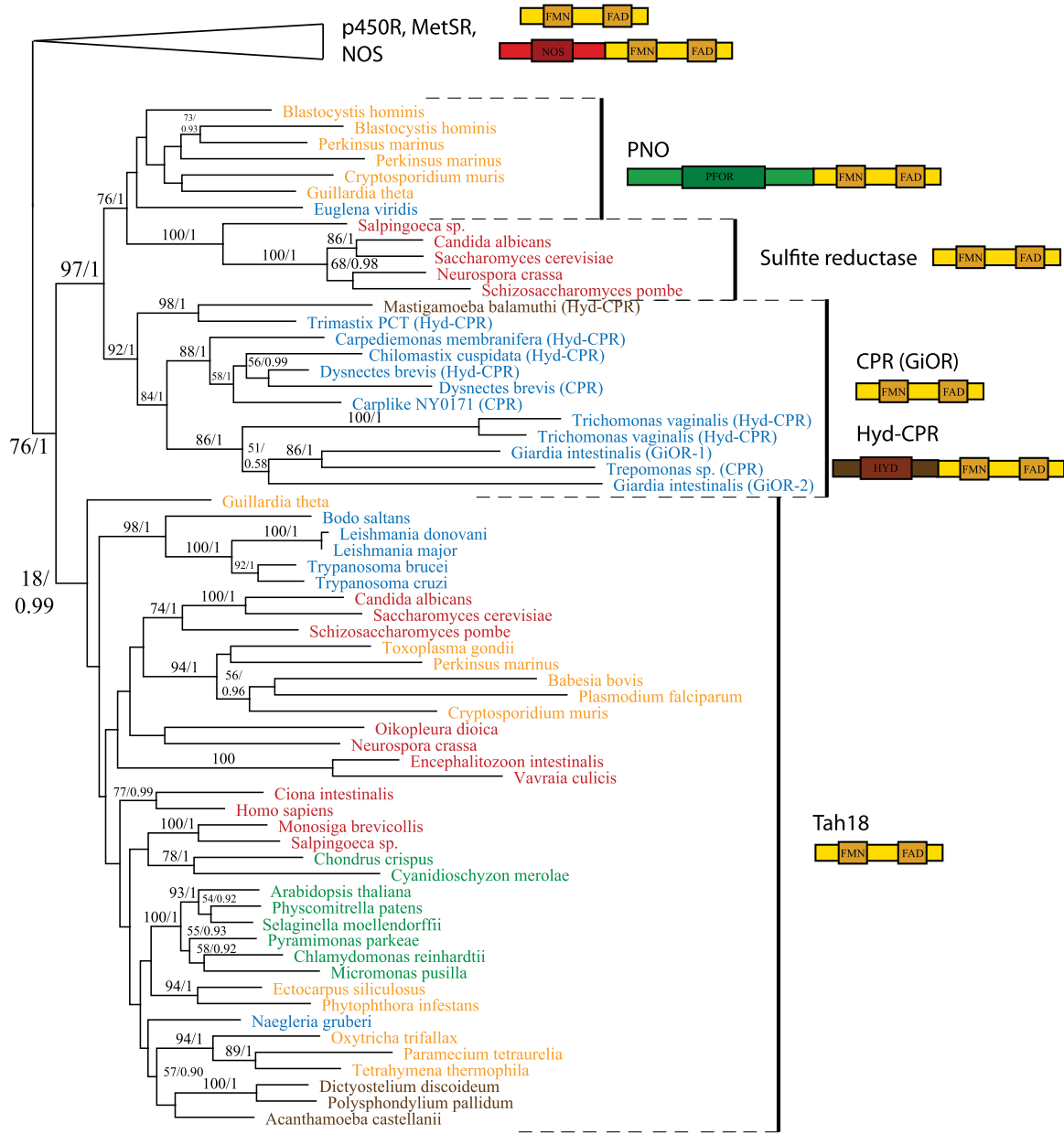


Fig. 5. Phylogeny of CPR domain containing proteins.

Maximum likelihood phylogeny of CPR domain containing proteins in eukaryotes. Numbers indicate statistical support in the form of bootstrap or PP values. The scale bar represents the estimated number of amino acid substitutions per site. Only bootstrap support and PP values greater than 50 and 0.5, respectively, are shown. p450 reductase (p450R), methionine synthase reductase (MetSR) and nitric oxide synthase (NOS) form distant branches of proteins. PNO, pyruvate NADP oxidoreductase; SR, Sulfite reductase alpha; CPR, CPR domain containing protein. Green indicates Viridiplantae, red Opisthokonta, yellow the SAR (Stramenopila, Apicomplexa, Rhizaria) supergroup, brown Amoebozoa, and blue Excavata. The schematic domain architecture for each protein group is displayed. PFOR, pyruvate:ferredoxin oxidoreductase domain; FMN, flavin mononucleotide binding domain; FAD, flavin adenine dinucleotide binding domain; HYD, hydrogenase domain.

Minimal cytosolic iron-sulfur cluster assembly (CIA) pathway of *G. intestinalis* comprises of Nbp35, Nar1, Cia1 and Cia2 proteins whereas essential electron donor Tah18/Dre2 complex, as well as Cfd1 and MMS19 seems to be absent in this parasite.

In addition to the cytosolic localization, Cia2 and Nbp35 are associated with mitosomes and might represent a novel connection between the mitochondrial FeS cluster assembly (ISC) and the CIA pathway.

is a subgroup of Excavata, resulted in the identification of only five of them (Nbp35, Cfd1, Nar1, Cia1 and Cia2; Fig. 1). Except for the putative MMS19 of *Trimastix*,

Dre2 and MMS19 are likely absent from Metamonada, a surprising finding for such a highly conserved and essential group of proteins. It is noteworthy that Dre2 is

usually absent from anaerobes (Basu *et al.*, 2013; Tsaousis *et al.*, 2014), and MMS19 has not been found in various members of Stramenophila, Apicomplexa, Viridiplantae and Microsporidia (Tsaousis *et al.*, 2014). Moreover, MMS19 is the only non-essential component of the *Arabidopsis thaliana* CIA machinery (Han *et al.*, 2015). Because Dre2 was recently implicated in the maturation of diferric-tyrosyl radical cofactor (Zhang *et al.*, 2014), we speculated whether the loss of Dre2 in anaerobes was reflected in the absence of the RNR2 proteins. However, because we did not find such correlation (Supporting Information Figure S3), it is unknown how cofactor of RNR2 is assembled in anaerobes.

The patchy distribution of Cfd1 in Metamonada implies multiple losses in *G. intestinalis* and *S. salmoneida* (Fig. 1). Because in plants, which appear to lack Cfd1, Nbp35 acts as a homodimer (Bych *et al.*, 2008), its similar function in these two metamonads is an interesting possibility. Furthermore, two key components of the mitochondrial export machinery, Erv1 and Atm1, are also likely absent in Metamonada. The recent finding that decreased enzymatic activities of cytosolic Fe-S proteins in the Erv1 yeast mutant strain are likely caused by glutathione depletion (Ozer *et al.*, 2015) questions the generally accepted role of Erv1 as a link between the ISC and CIA pathways (Lill, 2009). Because of its function as a cofactor of Atm1 (Srinivasan *et al.*, 2014), the tripeptide glutathione (GSH) is another putative player in cytosolic Fe-S synthesis (Sipos *et al.*, 2002). Interestingly, glutathione synthase and glutamate cysteine ligase, two proteins required for the synthesis of GSH, are present in the *G. intestinalis* genome (Morrison *et al.*, 2007). Additionally, in this protist, GSH was shown to be important for the stability of glutaredoxin 5 (Rada *et al.*, 2009). However, because GSH-synthesizing enzymes and glutaredoxins are absent from *T. vaginalis* and *S. salmoneida* (Carlton *et al.*, 2007; Xu *et al.*, 2014), it is unlikely that GSH plays any important role in the putative ISC and CIA connection in metamonads. The absence of Atm1 in these flagellates further supports this notion.

The CPR domain-containing proteins in metamonads appear to be non-orthologous to Tah18 protein (Tsaousis *et al.*, 2014). We postulate that they actually evolved from the CPR-hydrogenase fusion protein found in the common ancestor of metamonads (Fig. 5). Indeed, a similar scenario was proposed for GiOR-1 and GiOR-2 (Jedelsky *et al.*, 2011; Pyrih *et al.*, 2014), which cluster with PNO and the α -subunit of sulfite reductase (α -SR), the two of which are related proteins (Rotte *et al.*, 2001). Although a connection between GiORs and PNO had previously been suggested (Tsaousis *et al.*, 2014), it lacked statistical support. The architecture of these CPR-hydrogenase fusion proteins is unique for

metamonads. Despite its different origin, we cannot exclude the possibility that GiOR proteins might be functional Tah18 analogs in *G. intestinalis*. However, this is rather unlikely as Tah18 related activity is dependent on Dre2 (Netz *et al.*, 2010), which seems to be absent in metamonads. Interestingly, in a heterologous rescue, the GiOR proteins were able to restore the Fe-S cluster assembly in the Tah18-depleted procyclic stage of *T. brucei*. We propose that this phenomenon reflects a functional versatility of the CPR domain that enables several proteins to reduce various electron acceptors, such as Dre2, cytochrome p450 or methionine synthase (Netz *et al.*, 2010). Similarly, the previously reported reduction of cytosolic cytochrome *b*₅ by GiOR-1 (Pyrih *et al.*, 2014) appears to be nonphysiological because GiOR-1 is localized inside the mitosomes. Furthermore, artificial interaction with cytochromes was previously described for the human Tah18 homolog (Olteanu and Banerjee, 2003). Fe-S cluster assembly in mitosomes that is mediated by ISC machinery requires supply of electrons. Ferredoxin has been shown to be the main electron donor for ISC components. However, the metabolic source of electrons in mitosomes is unknown. We can speculate that GiOR-1 is somehow involved in electron transport associated with the function of ISC machinery. Previously, we tested an ability of GiOR-1 to transfer electrons to ferredoxin; however, we did not observe such an activity (Jedelsky *et al.*, 2011). Thus, the function of GiOR-1 remains unclear.

Intracellular localization of CIA components in *G. Intestinalis*

All known components of the CIA pathway in *G. intestinalis* are localized in the cytosol; however, Nbp35-1, Nbp35-2 and Cia2 are also associated with the mitosomes. Indeed, immunofluorescence microscopy shows that both Nbp35 proteins exhibit dual cytosolic and mitochondrial localization. However, only a small portion of each of them was found to be associated with the organellar fraction, as revealed by cell fractionation. The faint signal detected in the organellar fraction likely resulted from a transient interaction between Nbp35 and the mitosomes, which were disrupted during the fractionation procedure and washing steps. A similar phenomenon was observed in the case of Dre2, which is found throughout the cytosol as well as on the surface of yeast mitochondria (Peleh *et al.*, 2014).

To investigate the localization of Cia2 within the mitosome in greater detail, putative interacting proteins were subjected to precipitation, and the obtained lists of proteins were compared with those co-precipitated with other mitochondrial proteins (Martincová *et al.*, 2015). It is

worth noting that the majority of proteins pulled down by Cia2 were previously identified as partners of integral outer mitochondrial proteins Tom40 and GiMomp35, whereas only a slight overlap with lists of proteins obtained via mitochondrial matrix components GiOR-1, Pam18 and Tim44 was observed (Martincová *et al.*, 2015). Combined, the data obtained from subcellular fractionation and protease protection assay are compatible with Cia2 being localized both in the cytosol and in the intermembrane space of the mitosome.

Dual mitochondrial and cytosolic localization are not unprecedented for the CIA components; they were previously reported for Tah18 and Dre2 in yeast (Banci *et al.*, 2011). Tah18 is relocated from the cytosol to mitochondria upon the induction of oxidative stress conditions (Vernis *et al.*, 2009). A fraction of Dre2 is present in the mitochondrial intermembrane space and in the cytosol (Zhang *et al.*, 2008; Banci *et al.*, 2011), although this distribution was recently questioned by Peleh and colleagues, who suggested that the protein is present on the surface of the outer mitochondrial membrane (Peleh *et al.*, 2014). Whether mitochondrion-localized Tah18 and Dre2 play a role in the CIA pathway remains to be established. However, the dual localization reported herein for Nbp35 and Cia2 is novel. The recently described connection between Cia2 and plant mitochondria, reflected by unexpectedly reduced activity of mitochondrial aconitase along with an expected decrease in the activities of several Fe-S proteins in the cytosol (Luo *et al.*, 2012), may be particularly relevant in this context. In fact, any mechanism linking Cia2 and the ISC machinery remains unknown. The two human Cia2 proteins have different functions. Whereas CIA2B is responsible for the maturation of a wide range of nuclear and cytosolic Fe-S proteins, CIA2A is dedicated to the maturation of iron regulatory protein 1 (Stehling *et al.*, 2013). Homologs of both Cia2 variants are also present in the *T. brucei* genome, but no information is available regarding their function. It is tempting to speculate that *G. intestinalis* has solved the functional diversification of Cia2 by dual localization.

Possible connection between ISC and CIA pathways in *G. intestinalis*

In yeasts, plants and humans, the CIA pathway depends on the mitochondrial ISC pathway (Leighton and Schatz, 1995; Kispal *et al.*, 1999; Lange *et al.*, 2001; Mühlenhoff *et al.*, 2004). Although no data are available about such connection in metamonads, the best studied excavate protist *T. brucei* also appear to retain this arrangement (Horáková *et al.*, 2015). The ISC and protein import pathways are the only known ones identified within the

G. intestinalis mitosome (Jedelsky *et al.*, 2011; Martincová *et al.*, 2015). Counterintuitively, there is no known putative Fe-S protein in the mitosome apart from components of the ISC pathway itself, although several novel proteins have been recently identified in this highly reduced organelle (Martincová *et al.*, 2015). Therefore, one has to contemplate the possibility that the ISC pathway mediates the formation of Fe-S clusters for the extramitochondrial targets. Cysteine desulfurases catalyze the removal of sulfur from L-cysteine and are essential for all Fe-S cluster assembly pathways (Netz *et al.*, 2014), yet they were not found in the cytosol of any member of the Metamonada. Still, the activities of several Fe-S containing enzymes were measured in the cytosol of *G. intestinalis* (Townson *et al.*, 1996; Emelyanov and Goldberg, 2011). Therefore, it is plausible that in this group of diverged and reduced protists, the CIA machinery depends on the mitochondrial cysteine desulfurase (Tachezy *et al.*, 2001; Tovar *et al.*, 2003). The existence of paralogs of scaffold proteins Nbp35 on the surface of the mitosomes supports this assumption. Whether in *G. intestinalis* Cia2 partially substitutes for the function of the missing intermembrane space protein Erv1 and the inner membrane internal protein Atm1 will be the subject of future investigations.

In conclusion, our data suggest that *G. intestinalis* belongs to a handful of eukaryotes with CIA machinery lacking the electron donor complex Tah18/Dre2. Moreover, it is possible that this essential machinery is dependent on the mitochondrial ISC pathway, even in the absence of the well-characterized Atm1 and Erv1 linker proteins. We speculate that the scaffold proteins Nbp35-1 and Nbp35-2 located on the surface of the mitosome and the cluster delivery protein Cia2 in its intermembrane space might be components of this noncanonical connection. Additional research will be needed to support or disprove this interesting possibility.

Experimental procedures

Cultivation and transformation of *G. intestinalis*

Trophozoites of *G. intestinalis* strain WB (ATCC 30957) were grown in TY-S-33 medium (Keister, 1983) supplemented with 10% heat-inactivated bovine serum (PAA Laboratories), 0.1% bovine bile and antibiotics. For episomal expression, the CIA genes (GiardiaDB gene ID: GL50803_15324, GL50803_10969, GL50803_14604, GL50803_33030, GL50803_17550, GL50803_8819) were PCR-amplified and the amplicons were inserted into the plasmid pTG3039 (Lauwaet *et al.*, 2007), which was modified for the expression of proteins that contain the C-terminal hemagglutinin (HA) tag (Martincová *et al.*, 2015). The cells were transformed and selected as previously described (Singer *et al.*, 1998). Genes for co-

precipitation experiments (GL50803_8819 and GL50803_91252) were subcloned into pONDRA plasmid with a C-terminal BAP and coexpressed with the cytosolic BirA gene on pTG plasmid as previously described (Martincová *et al.*, 2015).

Immunofluorescence microscopy

G. intestinalis cells were fixed with 1% formaldehyde as described elsewhere (Dawson *et al.*, 2007). Proteins of interest were stained for immunofluorescence microscopy using α -HA tag rat monoclonal antibody (Roche). Additionally, we raised α -GiOR-1 rabbit polyclonal antibody and α -Nbp35-1 rat polyclonal antibody for the detection of GiOR-1 and Nbp35-1 proteins. α -TOM40 rabbit polyclonal antibody (Dagley *et al.*, 2009) and α -Grx5 polyclonal rat antibody (Rada *et al.*, 2009) were used as mitochondrial markers. Alexa Fluor 488 (green) donkey α -rat and α -rabbit antibodies and Alexa Fluor 594 (red) donkey α -rabbit and α -rat antibodies (Invitrogen) were used as secondary antibodies. Nuclei were stained with 4',6-diamidin-2-phenylindol (DAPI). The slides were examined using an Olympus IX81 microscope equipped with an MT20 illumination system, and the images were processed using ImageJ 1.41e software (NIH).

Preparation of subcellular fractions and immunoblot analysis

Giardia trophozoites were harvested, washed twice in phosphate-buffered saline (PBS), pH 7.4, and resuspended in SM buffer (250 mM sucrose and 20 mM morpholinepropanesulfonic acid, pH 7.2) supplemented with protease inhibitors (Complete EDTA-free Protease Inhibitor Cocktail; Roche). The cells were disrupted by sonication ($\sim 15 \times 1$ -s pulses) at an amplitude of 40 (Biorblock Scientific Vibra-Cell 72405) and centrifuged twice at 2,750g for 10 min to remove undisturbed cells. The supernatant was then centrifuged at 180,000g for 30 min to obtain the organellar fraction. Proteins were detected using the same sets of antibodies applied for immunofluorescence, and a signal was developed using corresponding secondary antibodies fused to alkaline phosphatase (Invitrogen). For protease protection assay, the organellar fraction (2 mg/ml) in SM buffer supplemented with protease inhibitors (Roche) was incubated with trypsin (200 μ g/ml) for 10 min at 37°C.

Coprecipitation of in vivo biotinylated proteins and their interacting partners

We used a strategy recently developed for the study of mitochondrial protein import machinery (Martincová *et al.*, 2015). Briefly, the organellar fraction (~ 10 mg) was resuspended in PBS (pH 7.4) at a final protein concentration of 1.5 mg/ml. The crosslinker DSP (Thermo Scientific) was then added (final concentration 25 μ M) and incubated for 1 h on ice. Following centrifugation at 30,000 \times g for 10 min at 4°C, the resulting pellet was resuspended in boiling buffer (50 mM Tris, 1 mM EDTA, 1% SDS, pH 7.4) and

incubated for 10 min at 80°C. The obtained supernatant was diluted 1:10 in incubation buffer (50 mM Tris, 150 mM NaCl, 5 mM EDTA, 1% Triton X 100; pH 7.4) supplemented with protease inhibitors. Then, 100 μ l of streptavidin coupled magnetic beads (Dynabeads® MyOne™ Streptavidin C1, Invitrogen) was mixed with the sample and incubated overnight at 4°C with gentle rotation. The beads were then washed in the following order (each step lasting 5 min): 3 times in incubation buffer, once in boiling buffer, once in washing buffer (60 mM Tris, 2% SDS, 10% glycerol) and twice in incubation buffer supplemented with 0.1% SDS. Finally, proteins were eluted from the beads in SDS PAGE sample buffer supplemented with 20 mM biotin for 5 min at 95°C. The eluate was resolved by SDS PAGE and stained with Coomassie brilliant blue. Separated proteins were destained, trypsin digested and analyzed by mass spectrometry. The same procedure was performed with wild-type *Giardia* and cells overexpressing BirA protein only, both used as negative controls.

Mass spectrometry

The trypsin digested proteins were loaded onto UltiMate 3000 RSLCnano system (Thermo Scientific - Dionex) coupled to a TripleTOF 5600 mass spectrometer with a NanoSpray III source (AB Sciex) for LC-MS/MS analysis. The instrument was operated with Analyst TF 1.6 (AB Sciex). TOF MS mass range was set to 350–1500 m/z, in MS/MS mode the instrument acquired fragmentation spectra within 100–2000 m/z. Spectra were searched against *G. intestinalis* database (GiardiaDB 28, <http://giardiadb.org/giardiadb/>), and the common contaminants database cRAP (<http://www.thegpm.org/crap/>) with Mascot 2.2. The results from Mascot were postprocessed with Percolator software (<http://percolator.ms/>) and resulting datasets were evaluated with the Scaffold software version 4.4.6 (Proteome Software, Portland) using False Discovery Rate (FDR) set to 1% for peptide and protein. All proteins identified in the negative controls (at least 95% protein identification probability) were subtracted from the dataset of immunoprecipitated proteins. Only proteins with 100% protein identification probability that were identified based on at least two peptides were considered as putative interactive proteins. The mass spectrometry proteomics data have been deposited to the ProteomeXchange Consortium via the PRIDE (Vizcaíno *et al.*, 2016) partner repository with the dataset identifier PXD004722.

Bioinformatic analyses

To classify the copurified proteins, their amino acid sequences were analyzed by BLASTP against the NCBI nr database and using the HHpred algorithm available at <http://toolkit.tuebingen.mpg.de/hhpred/> (Soding *et al.*, 2005). For phylogenetic analysis of Nar1 and CPR domain-containing proteins in eukaryotes, amino acid sequences were retrieved from a non-redundant GenBank protein database. EST sequences of various metamonads are available in SRA ncbi database under accession ID PRJNA315708. The sequences were aligned using the Mafft program

(Katoch *et al.*, 2002), and non-informative sites were removed using BMGE software (Criscuolo and Gribaldo, 2010). The best substitutional model (LG + G4 + I for both analyses) was calculated using the IQ tree program (Nguyen *et al.*, 2015), and phylogenetic analysis was performed using PhyML 3.0 (Guindon and Gascuel, 2003) and MrBayes (Huelsenbeck and Ronquist, 2001). Support values are shown next to the branches as the maximum-likelihood bootstrap support (PhyML) or posterior probabilities (MrBayes).

Rescue experiment in *T. brucei*

Procyclic *T. brucei* 29-13 were cultivated in SDM-79 medium (Carruthers and Cross, 1992) containing 10% fetal bovine serum, 15 µg/ml of geneticin and 50 µg/ml of hygromycin. The genes for GiOR-1 and GiOR-2 were cloned into pABPURO vector possessing an HA₃ tag. The resulting GiOR-1-pABPURO and GiOR-2-pABPURO constructs were linearized using NotI and electroporated individually into the TbTah18-TbDre2 RNAi double knock-down PS cells (Basu *et al.*, 2014) using a BTX electroporator, as described elsewhere (Vondrušková *et al.*, 2005). Positive transfectants were selected by clonal dilution using puromycin as a marker. In the presence of puromycin (1 µg/ml), RNAi was induced by the addition of tetracycline (1 µg/ml). Cell densities were measured using a Beckman Coulter Z2 counter every 24 h over a period of 10 days after induction. The cytosolic and mitochondrial fractions were obtained by digitonin fractionation (Šmíd *et al.*, 2006). Aconitase activity was in both subcellular compartments measured spectrophotometrically at 240 nm via the production of cis-aconitate from isocitrate (Long *et al.*, 2011).

Acknowledgements

The authors thank Frances Gillin (University of San Diego) for kindly providing plasmid pTG3039, and Jitka Štáfková for a critical reading of the manuscript. They thank Paul Michels (Universidad de los Andes/University of Edinburgh) and Alena Zíková (Institute of Parasitology, Biology Centre ASCR) for anti enolase and anti mtHsp70 antibodies, respectively. This work was supported by LQ1604 NPU II provided by MEYS, CZ.1.05/1.1.00/02.0109 BIOCEV provided by ERDF and MEYS to J.T., and the Czech Science Foundation 15-21974S provided to J.L. The work by M.K. and A.J.R. was supported by grant MOP-142349 from the Canadian Institutes of Health Research awarded to A.J.R.

References

- Balk, J., Pierik, A.J., Netz, D.J.A., Mühlenhoff, U., and Lill, R. (2004) The hydrogenase-like Nar1p is essential for maturation of cytosolic and nuclear iron-sulphur Proteins. *embo J* **23**: 2105–2115.
- Balk, J., Netz, D.J.A., Tepper, K., Pierik, A.J., and Lill, R. (2005) The essential WD40 protein Cia1 is involved in a late step of cytosolic and nuclear iron-sulfur protein assembly. *Mol Cell Biol* **25**: 10833–10841.
- Banci, L., Bertini, I., Ciolfi-Baffoni, S., Boscaro, F., Chatzi, A., Mikolajczyk, M., *et al.* (2011) Anamorsin is a [2Fe-2S] cluster-containing substrate of the Mia40-dependent mitochondrial protein trapping machinery. *Chem Biol* **18**: 794–804.
- Basu, S., Leonard, J.C., Desai, N., Mavridou, D.A.I., Tang, K.H., Goddard, A.D., *et al.* (2013) Divergence of Erv1-associated mitochondrial import and export pathways in Trypanosomes and anaerobic protists. *Eukaryot Cell* **12**: 343–355.
- Basu, S., Netz, D.J., Haindrich, A.C., Herlerth, N., Lagny, T.J., Pierik, A.J., *et al.* (2014) Cytosolic iron-sulphur protein assembly is functionally conserved and essential in procyclic and bloodstream *Trypanosoma brucei*. *Mol Microbiol* **93**: 897–910.
- Bych, K., Netz, D.J.A., Vigani, G., Bill, E., Lill, R., Pierik, A.J., and Balk, J. (2008) The essential cytosolic iron-sulfur protein Nbp35 acts without Cfd1 partner in the green lineage. *J Biol Chem* **283**: 35797–35804.
- Carlton, J.M., Hirt, R.P., Silva, J.C., Delcher, A.L., Schatz, M., Zhao, Q., *et al.* (2007) Draft genome sequence of the sexually transmitted pathogen *Trichomonas vaginalis*. *Science* **315**: 207–212.
- Carruthers, V.B. and Cross, G.A.M. (1992) High efficiency clonal growth of blood stream form and insect form *Trypanosoma brucei* on agarose plates. *Proc Natl Acad Sci U S A* **89**: 8818–8821.
- Criscuolo, A. and Gribaldo, S. (2010) BMGE (Block Mapping and Gathering with Entropy): A new software for selection of phylogenetic informative regions from multiple sequence alignments. *BMC Evol Biol* **10**: 210.
- Dagley, M.J., Doležal, P., Likic, V.A., Šmíd, O., Purcell, A.W., Buchanan, S.K., *et al.* (2009) The protein import channel in the outer mitochondrial membrane of *Giardia intestinalis*. *Mol Biol Evol* **26**: 1941–1947.
- Dawson, S.C., Sagolla, M.S., Mancuso, J.J., Woessner, D.J., House, S.A., Fritz-Laylin, L., and Cande, W.Z. (2007) Kinesin-13 regulates flagellar, interphase, and mitotic microtubule dynamics in *Giardia intestinalis*. *Eukaryot Cell* **6**: 2354–2364.
- Doležal, P., Šmíd, O., Rada, P., Zubáčová, Z., Bursac, D., Sutak, R., *et al.* (2005) *Giardia* mitochondria and trichomonad hydrogenosomes share a common mode of protein targeting. *Proc Natl Acad Sci U S A* **102**: 10924–10929.
- Emelyanov, V.V. and Goldberg, A.V. (2011) Fermentation enzymes of *Giardia intestinalis*, pyruvate:ferredoxin oxidoreductase and hydrogenase, do not localize to its mitochondria. *Microbiol SGM* **157**: 1602–1611.
- Gari, K., Ortiz, A.M.L., Borel, V., Flynn, H., Skehel, J.M., and Boulton, S.J. (2012) MMS19 links cytoplasmic Iron-Sulfur cluster assembly to DNA metabolism. *Science* **337**: 243–245.
- Guindon, S. and Gascuel, O. (2003) A simple, fast, and accurate algorithm to estimate large phylogenies by maximum likelihood. *Syst Biol* **52**: 696–704.
- Han, Y.F., Huang, H.W., Li, L., Cai, T., Chen, S., and He, X.J. (2015) The cytosolic iron-sulfur cluster assembly protein MMS19 regulates transcriptional gene silencing, DNA repair, and flowering time in Arabidopsis. *PLoS One* **10**:

- Hausmann, A., Netz, D.J.A., Balk, J., Pierik, A.J., Mühlenhoff, U., and Lill, R. (2005) The eukaryotic P loop NTPase Nbp35: An essential component of the cytosolic and nuclear iron-sulfur protein assembly machinery. *Proc Natl Acad Sci U S A* **102**: 3266–3271.
- Horáková, E., Changmai, P., Paris, Z., Salmon, D., and Lukeš, J. (2015) Simultaneous depletion of Atm and Mdl rebalances cytosolic Fe-S cluster assembly but not heme import into the mitochondrion of *Trypanosoma Brucei*. *febs J* **282**: 4157–4175.
- Huelsenbeck, J.P. and Ronquist, F. (2001) MRBAYES: Bayesian inference of phylogenetic trees. *Bioinformatics* **17**: 754–755.
- Iyanagi, T., Xia, C., and Kim, J.J. (2012) NADPH-cytochrome P450 oxidoreductase: Prototypic member of the diflavin reductase family. *Arch Biochem Biophys* **528**: 72–89.
- Jackson, A.P., Otto, T.D., Aslett, M., Armstrong, S.D., Bringaud, F., Schlacht, A., et al. (2016) Kinetoplastid phylogenomics reveals the evolutionary innovations associated with the origins of parasitism. *Curr Biol* **26**: 161–172.
- Jedelsky, P.L., Doležal, P., Rada, P., Pyrih, J., Šmíd, O., Hrdý, I., et al. (2011) The minimal proteome in the reduced mitochondrion of the parasitic protist *Giardia intestinalis*. *PLoS One* **6**: e17285.
- Katoh, K., Misawa, K., Kuma, K., and Miyata, T. (2002) MAFFT: A novel method for rapid multiple sequence alignment based on fast Fourier transform. *Nucl Acids Res* **30**: 3059–3066.
- Keister, D.B. (1983) Axenic culture of *Giardia lamblia* in Tyi-S-33 medium supplemented with bile. *Trans Roy Soc Trop Med Hyg* **77**: 487–488.
- Kispal, G., Csere, P., Prohl, C., and Lill, R. (1999) The mitochondrial proteins Atm1p and Nfs1p are essential for biogenesis of cytosolic Fe/S Proteins. *embo J* **18**: 3981–3989.
- Kolisko, M., Silberman, J.D., Cepicka, I., Yubuki, N., Takishita, K., Yabuki, A., et al. (2010) A wide diversity of previously undetected free-living relatives of diplomonads isolated from marine/saline habitats. *Environ Microbiol* **12**: 2700–2710.
- Kuhnke, G., Neumann, K., Mühlenhoff, U., and Lill, R. (2006) Stimulation of the ATPase activity of the yeast mitochondrial ABC transporter Atm1p by thiol compounds. *Mol Membr Biol* **23**: 173–184.
- Lange, H., Lisowsky, T., Gerber, J., Mühlenhoff, U., Kispal, G., and Lill, R. (2001) An essential function of the mitochondrial sulfhydryl oxidase Erv1p/ALR in the maturation of cytosolic Fe/S proteins. *EMBO Rep* **2**: 715–720.
- Lauwaet, T., Davids, B.J., Torres-Escobar, A., Birkeland, S.R., Cipriano, M.J., Preheim, S.P., et al. (2007) Protein phosphatase 2A plays a crucial role in *Giardia lamblia* differentiation. *Mol Biochem Parasitol* **152**: 80–89.
- Leighton, J. and Schatz, G. (1995) An ABC transporter in the mitochondrial inner membrane is required for normal growth of Yeast. *embo J* **14**: 188–195.
- Lill, R. (2009) Function and biogenesis of iron-sulphur proteins. *Nature* **460**: 831–838.
- Lill, R., Dutkiewicz, R., Freibert, S.A., Heidenreich, T., Mascarenhas, J., Netz, D.J., et al. (2015) The role of mitochondria and the CIA machinery in the maturation of cytosolic and nuclear iron-sulfur proteins. *Eur J Cell Biol* **94**: 280–291.
- Long, S.J., Changmai, P., Tsaousis, A.D., Skalicky, T., Verner, Z., Wen, Y.Z., et al. (2011) Stage-specific requirement for Isa1 and Isa2 proteins in the mitochondrion of *Trypanosoma brucei* and heterologous rescue by human and *Blastocystis* orthologues. *Mol Microbiol* **81**: 1403–1418.
- Luo, D.X., Bernard, D.G., Balk, J., Hai, H., and Cui, X.F. (2012) The DUF59 family gene AE7 acts in the cytosolic Iron-Sulfur cluster assembly pathway to maintain nuclear genome integrity in Arabidopsis. *Plant Cell* **24**: 4135–4148.
- Martincová, E., Voleman, L., Pyrih, J., Žársk, V., Vondráčková, P., Kolisko, M., et al. (2015) Probing the biology of *Giardia intestinalis* mitosomes using in vivo enzymatic tagging. *Mol Cell Biol* **35**: 2864–2874.
- Morrison, H.G., McArthur, A.G., Gillin, F.D., Aley, S.B., Adam, R.D., Olsen, G.J., et al. (2007) Genomic minimalism in the early diverging intestinal parasite *Giardia lamblia*. *Science* **317**: 1921–1926.
- Mühlenhoff, U., Balk, J., Richhardt, N., Kaiser, J.T., Sipos, K., Kispal, G., and Lill, R. (2004) Functional characterization of the eukaryotic cysteine desulfurase Nfs1p from *Saccharomyces cerevisiae*. *J Biol Chem* **279**: 36906–36915.
- Netz, D.J.A., Pierik, A.J., Stumpfig, M., Mühlenhoff, U., and Lill, R. (2007) The Cfd1-Nbp35 complex acts as a scaffold for iron-sulfur protein assembly in the yeast cytosol. *Nat Chem Biol* **3**: 278–286.
- Netz, D.J.A., Stumpfig, M., Dore, C., Mühlenhoff, U., Pierik, A.J., and Lill, R. (2010) Tah18 transfers electrons to Dre2 in cytosolic iron-sulfur protein biogenesis. *Nat Chem Biol* **6**: 758–765.
- Netz, D.J.A., Pierik, A.J., Stumpfig, M., Bill, E., Sharma, A.K., Pallesen, L.J., et al. (2012) A bridging [4Fe-4S] cluster and nucleotide binding are essential for function of the Cfd1-Nbp35 complex as a scaffold in Iron-Sulfur protein maturation. *J Biol Chem* **287**: 12365–12378.
- Netz, D.J.A., Mascarenhas, J., Stehling, O., Pierik, A.J., and Lill, R. (2014) Maturation of cytosolic and nuclear iron-sulfur proteins. *Trends Cell Biol* **24**: 303–312.
- Nguyen, L.T., Schmidt, H.A., von Haeseler, A., and Minh, B.Q. (2015) IQ-TREE: A fast and effective stochastic algorithm for estimating maximum-likelihood phylogenies. *Mol Biol Evol* **32**: 268–274.
- Nishimura, A., Kawahara, N., and Takagi, H. (2013) The flavoprotein Tah18-dependent NO synthesis confers high-temperature stress tolerance on yeast cells. *Biochem Biophys Res Commun* **430**: 137–143.
- Nývltová, E., Stairs, C.W., Hrdý, I., Rídl, J., Mach, J., Pačes, J., et al. (2015) Lateral gene transfer and gene duplication played a key role in the evolution of *Mastigamoeba balamuthi* hydrogenosomes. *Mol Biol Evol* **32**: 1039–1055.
- Olteanu, H. and Banerjee, R. (2003) Redundancy in the pathway for redox regulation of mammalian methionine synthase - Reductive activation by the dual flavoprotein, novel reductase 1. *J Biol Chem* **278**: 38310–38314.
- Ozer, H.K., Dlouhy, A.C., Thornton, J.D., Hu, J., Liu, Y., Barycki, J.J., et al. (2015) Cytosolic Fe-S cluster protein

- maturation and iron regulation are independent of the mitochondrial Erv1/Mia40 import system. *J Biol Chem* **290**: 27829–27840.
- Peleh, V., Riemer, J., Dancis, A., and Herrmann, J.M. (2014) Protein oxidation in the intermembrane space of mitochondria is substrate-specific rather than general. *Microbial Cell* **1**: 81–93.
- Peters, J.W., Lanzilotta, W.N., Lemon, B.J., and Seefeldt, L.C. (1998) X-ray crystal structure of the Fe-only hydrogenase (Cpl) from *Clostridium pasteurianum* to 1.8 angstrom resolution. *Science* **282**: 1853–1858.
- Pyrih, J., Harant, K., Martinová, E., Sutak, R., Lesuisse, E., Hrdý, I., and Tachezy, J. (2014) *Giardia intestinalis* incorporates heme into cytosolic cytochrome b(5). *Eukaryot Cell* **13**: 231–239.
- Rada, P., Šmíd, O., Sutak, R., Doležal, P., Pyrih, J., Žárský, V., et al. (2009) The monothiol single-domain glutaredoxin is conserved in the highly reduced mitochondria of *Giardia intestinalis*. *Eukaryot Cell* **8**: 1584–1591.
- Rotte, C., Stejskal, F., Zhu, G., Keithly, J.S., and Martin, W. (2001) Pyruvate: NADP(+) oxidoreductase from the mitochondrion of *Euglena gracilis* and from the apicomplexan *Cryptosporidium parvum*: A biochemical relic linking pyruvate metabolism in mitochondriate and amitochondriate protists. *Mol Biol Evol* **18**: 710–720.
- Singer, S.M., Yee, J., and Nash, T.E. (1998) Episomal and integrated maintenance of foreign DNA in *Giardia lamblia*. *Mol Biochem Parasitol* **92**: 59–69.
- Sipos, K., Lange, H., Fekete, Z., Ullmann, P., Lill, R., and Kispal, G. (2002) Maturation of cytosolic iron-sulfur proteins requires glutathione. *J Biol Chem* **277**: 26944–26949.
- Šmíd, O., Horáková, E., Vilímová, V., Hrdý, I., Cammack, R., Horvath, A., et al. (2006) Knock-downs of iron-sulfur cluster assembly proteins IscS and IscU down-regulate the active mitochondrion of procyclic *Trypanosoma brucei*. *J Biol Chem* **281**: 28679–28686.
- Soding, J., Biegert, A., and Lupas, A.N. (2005) The HHpred interactive server for protein homology detection and structure prediction. *Nucl Acids Res* **33**: W244–W248.
- Srinivasan, V., Pierik, A.J., and Lill, R. (2014) Crystal structures of nucleotide-free and glutathione-bound mitochondrial ABC transporter Atm1. *Science* **343**: 1137–1140.
- Stehling, O., Vashisht, A.A., Mascarenhas, J., Jonsson, Z.O., Sharma, T., Netz, D.J.A., et al. (2012) MMS19 assembles iron-sulfur proteins required for DNA metabolism and genomic integrity. *Science* **337**: 195–199.
- Stehling, O., Mascarenhas, J., Vashisht, A.A., Sheftel, A.D., Niggemeyer, B., Rosser, R., et al. (2013) Human Cia2A-Fam96A and Cia2B-Fam96B integrate iron homeostasis and maturation of different subsets of cytosolic-nuclear Iron-Sulfur proteins. *Cell Metabol* **18**: 187–198.
- Tachezy, J., Sanchez, L.B., and Müller, M. (2001) Mitochondrial type iron-sulfur cluster assembly in the amitochondriate eukaryotes *Trichomonas vaginalis* and *Giardia intestinalis*, as indicated by the phylogeny of IscS. *Mol Biol Evol* **18**: 1919–1928.
- Takishita, K., Kolisko, M., Komatsuzaki, H., Yabuki, A., Inagaki, Y., Čepička, I., et al. (2012) Multigene phylogenies of diverse Carpediemonas-like organisms identify the closest relatives of 'Amitochondriate' Diplomonads and Retortamonads. *Protist* **163**: 344–355.
- Tanaka, N., Kanazawa, M., Tonosaki, K., Yokoyama, N., Kuzuyama, T., and Takahashi, Y. (2015) Novel features of the ISC machinery revealed by characterization of *Escherichia coli* mutants that survive without iron-sulfur clusters. *Mol Microbiol* **99**: 835–848.
- Tovar, J., Leon-Avila, G., Sanchez, L.B., Sutak, R., Tachezy, J., van der Giezen, M., et al. (2003) Mitochondrial remnant organelles of *Giardia* function in iron-sulphur protein maturation. *Nature* **426**: 172–176.
- Townson, S.M., Upcroft, J.A., and Upcroft, P. (1996) Characterisation and purification of pyruvate:ferredoxin oxidoreductase from *Giardia duodenalis*. *Mol Biochem Parasitol* **79**: 183–193.
- Tsaousis, A.D., Gentekaki, E., Eme, L., Gaston, D., and Roger, A.J. (2014) Evolution of the cytosolic iron-sulfur cluster assembly machinery in Blastocystis species and other microbial eukaryotes. *Eukaryot Cell* **13**: 143–153.
- Vernis, L., Facca, C., Delagoutte, E., Soler, N., Chanet, R., Guiard, B., et al. (2009) A newly identified essential complex, Dre2-Tah18, controls mitochondria integrity and cell death after oxidative stress in yeast. *PLoS One* **4**:
- Vizcaíno, J.A., Csordas, A., del-Toro, N., Dianes, J.A., Griss, J., Lavidas, I., et al. (2016) 2016 update of the PRIDE database and related tools. *Nucleic Acids Res* **44**: D447–D456.
- Vondrušková, E., van den Burg, J., Zíková, A., Ernst, N.L., Stuart, K., Benne, R., and Lukeš, J. (2005) RNA interference analyses suggest a transcript-specific regulatory role for mitochondrial RNA-binding proteins MRP1 and MRP2 in RNA editing and other RNA processing in *Trypanosoma brucei*. *J Biol Chem* **280**: 2429–2438.
- Weerapana, E., Wang, C., Simon, G.M., Richter, F., Khare, S., Dillon, M.B.D., et al. (2010) Quantitative reactivity profiling predicts functional cysteines in proteomes. *Nature* **468**: 790–U79.
- Xu, F.F., Jerlstrom-Hultqvist, J., Einarsson, E., Astvaldsson, A., Svard, S.G., and Andersson, J.O. (2014) The genome of *Spironucleus salmonicida* highlights a fish pathogen adapted to fluctuating environments. *PLoS Genetics* **10**:
- Zhang, Y., Lyver, E.R., Nakamaru-Ogiso, E., Yoon, H., Amutha, B., Lee, D.W., et al. (2008) Dre2, a conserved eukaryotic Fe/S cluster protein, functions in cytosolic Fe/S protein biogenesis. *Mol Cell Biol* **28**: 5569–5582.
- Zhang, Y., Li, H.R., Zhang, C.G., An, X.X., Liu, L.L., Stubbe, J., and Huang, M.X. (2014) Conserved electron donor complex Dre2-Tah18 is required for ribonucleotide reductase metallocofactor assembly and DNA synthesis. *Proc Natl Acad Sci U S A* **111**: E1695–E1704.

Supporting information

Additional supporting information may be found in the online version of this article at the publisher's web-site.